Biomedical Signal Processing and Control 62 (2020) 102103

Contents lists available at ScienceDirect

Biomedical Signal Processing and Control

journal homepage: www.elsevier.com/locate/bspc

Research Paper

Optimal imaging of multi-channel EEG features based on a novel clustering technique for driver fatigue detection

Chi Zhang [a,d,*], Lina Sun [a], Fengyu Cong [a,b,c,d], Tuomo Kujala [b], Tapani Ristaniemi [b], Tiina Parviainen [e]

[a] School of Biomedical Engineering, Faculty of Electronic Information and Electrical Engineering, Dalian University of Technology, Dalian 116024, China
[b] Faculty of Information Technology, University of Jyvaskyla, Mattilanniemi 2, Jyvaskyla FIN-40014, Finland
[c] School of Artificial Intelligence, Faculty of Electronic Information and Electrical Engineering, Dalian University of Technology, Dalian, 116024, China
[d] Liaoning Key Laboratory of Integrated Circuit and Biomedical Electronic System, Dalian University of Technology, Dalian, 116024, China
[e] Department of Psychology, University of Jyvaskyla, Kärki, Mattilanniemi 6, Jyvaskyla FI-40014, Finland

ARTICLE INFO

Keywords:
Fatigue detection
EEG
Signal processing
Brain network
Clustering

ABSTRACT

Fatigue may cause a decrease in mental and physical performance capacity, which is a serious safety risk for the drivers in the transportation system. Recently, various studies have demonstrated the deviations of electroencephalogram (EEG) indicators from normal vigilant state during fatigue in time and frequency domains. However, when considering spatial information, these feature descriptors are not satisfying the demand for reliable detection due to the well-known challenge of signal mixing. In this paper, we propose a novel approach based on clustering on brain networks (CBNs) to alleviate the problem to improve the performance of driver fatigue detection. The clustering algorithm was employed to extract the spatial nodes with distinct connectivity attributes throughout the EEG-based brain networks. Then, the temporal features of wavelet entropy from the extracted nodes were transformed to spatio-temporal images so that the image edge detection method (pulse-coupled neural networks) to distinguish different stages of fatigue can be used. The experimental results demonstrated the temporal features from the extracted nodes reduced signal mixing and showed clearer deviations. The detected fatigue based on the imaging method was to an extent consistent with self-reported subjective feelings and most of the critical fatigue was detected before the subjective feelings of fatigue. For all the subjects, 21 of 29 accidents happened after detected fatigue in the simulated driving task. Therefore, the proposed method owns potential value for early warning and avoidance of traffic accidents caused by driver fatigue.

1. Introduction

Fatigue decreases drivers' ability to operate vehicles safely and reduces their alertness level. It is one of the most important contributors to road accidents [1,2]. According to a report from National Highway Traffic Safety Administration (NHTSA), the accidents caused by driver fatigue make up close to 16.5 % of fatal crashes, but more than 1 in 4 drivers (29.4 %) reported having driving experience when they were so tired that they had a hard time keeping their eyes open in the past 30 days [3]. Thus, how to quantify, assess, and mitigate driver fatigue based on objective measurements, is an important challenge for traffic safety research [4,5]. Electrophysiology-based detection extracts the non-visible characteristics including heart rate variability, electrooculogram (EOG), electromyogram (EMG), and electroencephalogram (EEG), as well as other physiological indexes, reflecting the change of the physiological states directly and reliably [1,6–8]. In particular, EEG, which directly reflects the activities of the human brain is sensitive to fluctuations in alertness and has been applied to predicting performance degradation in a prolonged driving task [9].

As a physiological process which is gradual and accumulative, mental fatigue usually involves a number of different stages from the alertness and vigor stage to the tiredness and weakness state [4]. Correspondingly, its promising indicator, EEG, has demonstrated stage changes with state-specific and frequency-specific topographical

* Corresponding author.
E-mail addresses: chizhang@dlut.edu.cn (C. Zhang), lnsun@dlut.edu.cn (L. Sun), cong@dlut.edu.cn (F. Cong), tuomo.j.kujala@jyu.fi (T. Kujala), tapani.e.ristaniemi@jyu.fi (T. Ristaniemi), tiina.m.parviainen@jyu.fi (T. Parviainen).

https://doi.org/10.1016/j.bspc.2020.102103
Received 11 February 2020; Received in revised form 4 July 2020; Accepted 21 July 2020
Available online 15 August 2020

differences in the fatigue transition [10,11]. According to the EEG differences, driver fatigue can be effectively identified by classification algorithms to make timely warning instructions. Currently, most of the existing methods detect driver fatigue based on the differences in the time and frequency domains. The detection accuracy of state-of-the-art techniques has exceeded 90 %. In the frequency domain, previous studies have shown that increasing drowsiness is typically associated with progressive changes in rhythmic activities, such as theta (4–8 Hz), alpha (8–13 Hz), or beta (13–30 Hz) activity or their combinations (e.g. (theta + alpha)/beta) [8,12]. Hence, these spectral features have been extracted to develop driver fatigue detection systems. For example, Li et al. [13] calculated 12 types of power spectra combinations of the rhythmic activities and fed them into the linear regression modal, which achieved an accuracy of 91.5 % for fatigue detection. At present, alpha-based analysis is a relatively most efficient method for detecting driver fatigue in frequency domain. The power of alpha oscillations predominantly in the central and posterior brain regions (parieta-l-occipital) is generally increased when the subjects are fatigued or tired [6,12]. According to the burst of alpha activity [8], Lawhern et al. [14] developed a discounted autoregressive (DAR) method just depending on the statistical properties of the alpha frequency band and achieved approximately 95 % accuracy.

Since the degraded performance of fatigue is involved in a variety of brain activity changes, the EEG complexity that can be quantified by different entropy estimators has been regarded as another prominent feature [5,15,16]. Through entropy-based feature extraction, the system realized the nonlinear estimation of the dynamical EEG activity during driving [5]. The typical entropy estimators used in fatigue detection system are fuzzy entropy (FE) [17] and wavelet entropy (WE) [18]. On the basis of FZ analysis, Luo et al. [19] introduced an adaptive scaling factor and proposed adaptive multi-scale FZ. It increased the detection accuracy to 95.4 %. In [5], the researchers explored WE-based real-time feature extraction of driver fatigue by using sliding window and analyzed the fusion effects of WE, approximate entropy (ApEn), sample entropy (SampEn). When these entropy features were applied to the multilayer perceptron (MLP) neural network, it achieved 96.5 % accuracy.

In accordance with the ten-twenty international standards [20], EEG signals are recorded from multiple electrodes attached to the scalp with a fixed spatial arrangement. Among the fatigue detection methods mentioned above, the EEG analyses in the time and frequency domains may neglect the valuable correlation information of the signals from different electrode positions, which can be concretely interpreted as a spatial domain.

As pointed out in the literature [21], a fatigued driver may fail to functionally and fast enough engage multi-perceptual and processing functions (e.g. attention, reasoning, decision making, sensorimotor coordination, and visual processing), resulting in a series of risky driving behaviors. The coherence and interaction between distinct brain resources intuitively appear to be important for these functions. As a technological advancement in neuroscience, functional brain network analysis, measuring coupling of the functional activities in different brain regions, can provide richer information about human cognition than simpler univariate approaches [22,23]. Several studies have reported that the functional brain networks become more integrated during task performance in comparison with the resting state, but linearly decline with ongoing time-on-task [23,24]. In the prolonged visuomotor vigilance task, Gaggioni et al. [25] suggested that decreased propagation of EEG response evoked by transcranial magnetic stimulation within the fronto-parietal cortex was related to the failure of increased vigilance. Under the simulated driving condition, Kong et al. [26] also revealed the degraded performance of small-world features of brain networks under fatigue state, providing further support for the presence of a reshaped global topology in connectivity networks when drivers shifted from the alert to the drowsy stage. Zhao et al. [27] attributed the shift to a more economic but less efficient configuration, or an inability to retrieve these resources related to mental fatigue.

However, when the spatial connectivity analysis are directly applied to fatigue detection, it may encounter challenges, because of signal mixing. Signal mixing also translates to volume conduction in the case of EEG recordings. This problem is caused by that the activity of any single neuronal source is detected by a spatially widespread group of electrodes. Therefore, the brain networks may contain spurious interactions [28,29]. It is difficult to find the related electrodes which are the most sensitive to the degraded performance to optimize fatigue detection.

In this context, we propose a novel EEG signal analysis approach based on clustering on brain networks (CBNs) to get more reliable and sensitive information from both the spatial and temporal dimensions to detect driver fatigue. Our hypothesis is that the introduced spatial information through CBNs can further improve the detection accuracy. The entire framework and its application are shown in Figs. 1 and 2. In order to alleviate the problem of signal mixing, connection cluster is considered as the basic unit of connectivity analysis in CBNs. A connection cluster is defined as a tree composed of a node and the connections linking to it so that we can keep the effective information on fewer significant nodes with the similar links after clustering. Then, the EEG nonlinear dynamical features are extracted on the significant nodes (electrodes). Since the features on the significant nodes have consistent staged changes, the corresponding feature matrices are converted into images and we employ the image edge detection method to distinguish different stages of fatigue.

This paper is organized as follows. In Section 2, we describe the experimental details and EEG data preprocessing (see Sections 2.1 and 2.2), elaborate CBNs applied to suppress signal mixing to find significant nodes (see Section 2.3), add temporal feature extraction on the significant nodes to form imaging feature matrices (see Section 2.4), and illustrate two-dimensional pattern recognition to distinguish different stages of fatigue (see Section 2.5). Results of the study are presented in Section 3 and discussed in 4. Finally, the paper concludes in Section 5.

2. Materials and methods

2.1. Experiments and data

This study was reviewed and approved by Ethics Committee, Dalian

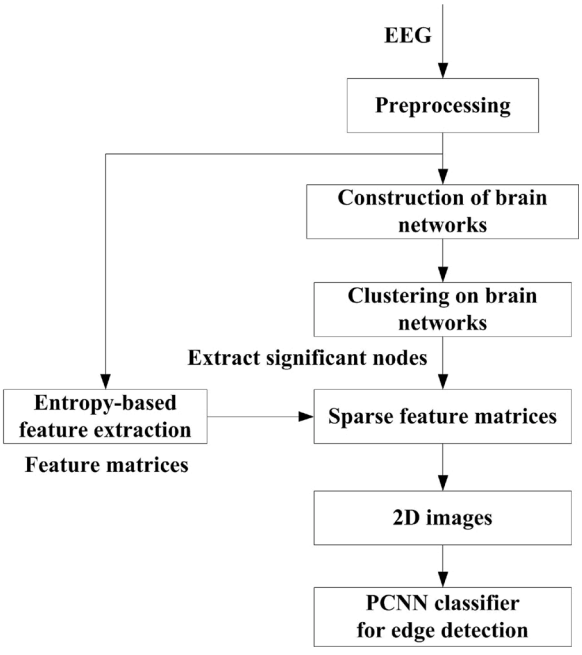

Fig. 1. Block diagram of the entire system.

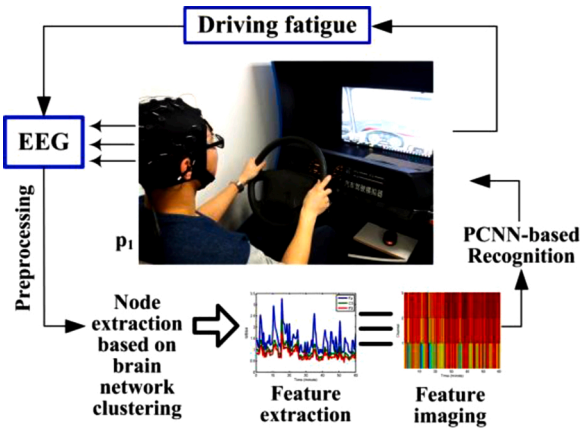

Fig. 2. Experimental setting and application of driver fatigue detection.

University of Technology (protocol number: 2018−040). Written informed consents were obtained from all participants before the experiments. Sixteen healthy right-handed subjects (eight males and eight females, age range: 20–35) who had driving licenses were recruited to participate in the simulated driving experiments. All the subjects had normal intelligence and no mental disorders or sleep problems. They have the habit of taking a nap after lunch. To induce fatigue in a short time, we deprived them of their nap and the experiments were conducted during 13 : 00∼15 : 00 after lunch. During the experiments, they were asked to refrain from taking any type of medicine and irritating drinks such as alcohol, coffee or tea. Each subject drove along for more than one hour under monotonous highway environment produced in a driving simulator (see Fig. 2). The driving simulator mainly consisted of a cockpit, a host computer, a CRT monitor, an audio system, operating sensors, and a data collector. The cockpit contained the same operational components as the real vehicle, such as a steering wheel, a clutch, a foot brake, an accelerator pedal and a hand brake. The simulator had both automatic and manual transmission (including five forward gears and one reverse gear). To reduce the movements of the subjects and make the task boring, we asked the subjects to drive using automatic transmission. As pointed out in [30,31], the simulators output vehicle control parameters, which can be used for learning driver behaviour. In the prolonged driving task, we recorded the self-reported moments of fatigue provided by the subjects' real-time feedback for method validation. Considering cumulative fatigue effect, subsequent self-reports were marked with the labels of higher fatigue levels. Accidents are allowed to occur during simulated driving under the condition of ensuring driver safety, which is different from real-world driving. Every event that went out of control was defined as an accident such as crash, contact with partition wall and driving in the off-road. The accident occurrence time was recorded for validation. Only the datasets with the accident EEG were adopted. All the subjects provided definite judgment on their fatigue (see Table 1 and Fig. 10) and accidents happened in the experiments. Nineteen standard electrodes (i.e. Fp1, Fp2, F7, F3, Fz, F4, F8, T3, C3, Cz, C4, T4, T5, P3, Pz, P4, T6, O1, and O2) mounted on a cap (NuAmps, Neuroscan) were attached to the scalps following the International 10–20 System to collect the drivers' EEG data. The EEG's sampling frequency is 500 Hz.

Table 1
Subject's subjective markings.

Fatigue level	1	2	3
Time (minute) marked by the subject	16.13	20.97	27.90
Time (minute) determined by PCNN	18.50	25.50	27.00

2.2. Data preprocessing

As mentioned above, rhythmic alpha activity has an outstanding performance for the fatigue analysis in the frequency domain. The raw EEG data (Fig. 3(a)) were filtered with a wavelet transform method (see [5]) between 7.8–15.6 Hz to obtain the rough alpha oscillation (Fig. 3 (b)). The wavelet transform method has the advantage of good local representation in both time and frequency domains compared to Fourier transform, so it is applied to the rhythm extraction to keep the critical information, although the frequency band is dichotomous. Further, a wavelet-based threshold technique which has been shown to be effective by Kar et al. [4] was utilized to correct the rough alpha wave, since the alpha wave was still affected by remaining artifacts (in the red box in Fig. 3(b)) that might seriously affect dynamic feature extraction. If any of the wavelet coefficients C in alpha band was greater than the threshold about mean and standard deviation mean(C)+2*std(C), it was halved to reduce the impact of artifacts. Then the wavelet-corrected EEG signal (Fig. 3(c)) was obtained by reconstruction from the processed coefficients.

2.3. Clustering on brain networks

According to graph theory [32], a brain network can be represented by a graph G(**N**, **E**) where **N** and **E** are the node and edge sets respectively. We assigned EEG electrodes to the nodes of G(**N**, **E**). The edges reflecting the adjacency relations among the nodes in the networks can be described by the adjacency matrix $\boldsymbol{A}$ whose element $\boldsymbol{A}(i, j)$ shows the edge between electrodes (nodes) i and j. In the fatigue detection application, we adopted the cross-correlation function [33] which is a simple and most commonly used measure of the connectivity to quantify the adjacency relations in $\boldsymbol{A}$. The correlation between the EEG signals s_i and s_j can be calculated by the following equations.

$$\gamma_{ij} = \left| \frac{CC(s_i, s_j)(\tau)}{\sqrt{CC(s_i, s_i)(0)CC(s_j, s_j)(0)}} \right| \tag{1}$$

$$CC(s_i, s_j)(\tau) = \begin{cases} \sum_{t-1}^{N-\tau} s_i(t+\tau)s_j(t) & \tau \geq 0 \\ CC(s_j, s_i)(\tau) & \tau < 0 \end{cases} \tag{2}$$

where time delay τ is set to 0. γ_{ij} is corresponding to the element of the adjacency matrix $\boldsymbol{A}$, which presents in ith row and jth column. To exclude self-connections of nodes, the elements on the main diagonal of $\boldsymbol{A}$ were set to zero. The other elements of $\boldsymbol{A}$ reflect functional interactions among brain signals reflected by different electrodes.

Considering the spatial fluctuations that may blur the critical time-course information (see Fig. 8), we employed an unsupervised

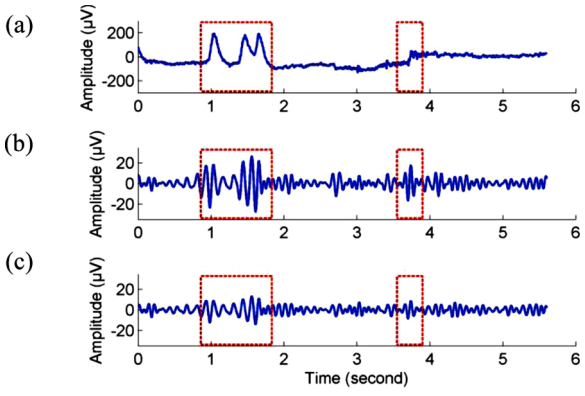

Fig. 3. Preprocessing of original EEG signal. (a) Original EEG signal. (b) Alpha rhythms extracted by wavelet decomposition. (c) Corrected EEG signal.

clustering algorithm to search the nodes with the significant connectivity information in the constructed brain networks. Since every connection cluster only has a node, classification of these clusters is to classify nodes in a brain network. The connections of a connection cluster are defined as the attributes of its node thereafter.

Mathematically, we re-express the brain network G(**N**, **E**) with N nodes as $\boldsymbol{X}=\{\boldsymbol{X}_1, \boldsymbol{X}_2, \ldots, \boldsymbol{X}_N\}^{\mathrm{T}}$, where $\boldsymbol{X}_i=\{x_i^1, x_i^2, \ldots, x_i^M\}$ with M links (M=N-1 for weighted network) is a vector denoting the ith node whose attribute $x_i^j = A(i,j)$ ($j \neq i$) is a scalar representing the strength of the functional connectivity between Node i and Node j. The spatial connectivity information is searched based on agglomerative hierarchical clustering, which establishes the foundations for inducing a hierarchical clustering from a newly represented, or newly encoded, mapping of functional connectivity matrix $\boldsymbol{A}$.

Fig. 4 shows the clustering process of the brain network with 5 nodes (5 connection clusters). To begin with, each node and its attributes in a brain network (represented by the network of EEG electrodes) is considered as a single-element cluster at the lowest level, i.e. $C_i=\{X_i\}$, $1 \leq i \leq N$. $\textbf{Dendrogram}_k = \{C_1, C_2, \ldots, C_N\}$, $k=N$. Then, based on the distance (similarity function) calculation, two closest clusters are successively merged to reduce the number of clusters by 1 until a single cluster remains at the highest level (i.e. $k=1$).

$$(a,b) = argmin_{(i,j)}\{d(C_i, C_j) : 1 \leq i < j \leq k\} \tag{3}$$

$$\mathrm{merge}(C_a, C_b) = C_{2N+1-k} \tag{4}$$

$$Dendrogram_{k-1} = Dendrogram_k - \{C_a, C_b\} + \{C_{2N+1-k}\} \tag{5}$$

where C_i and C_j denote two different clusters; k is the level number; **Dendrogram** indicates the cluster set and its element number is reduced by 1 to reach a higher level in Eq. (5); and d represents Euclidean distance between two clusters. This Euclidean distance can be calculated by the following expressions:

$$d(C_i, C_j) = d(X_a, X_b) \tag{6}$$

$$d(X_a, X_b) = \sqrt{\sum_{m=1}^{M} \left(x_a^m - x_b^m\right)^2} \tag{7}$$

where M denotes the number of attributes of the node vectors $\boldsymbol{X}_a$ and $\boldsymbol{X}_b$. x_a^m and x_b^mindicate the attributes (corresponding to functional connectivity) of the two node vectors.

Finally, we cut the dendrogram to complete clustering on brain networks to obtain different node groups of which number (Z) is predetermined. As the number of the clusters contained in **Dendrogram** is equal to the level number k, Z clusters will be left by the Zth level cut through the dendrogram. That means we classify the nodes of the brain networks into Z groups according to the elements (clusters) of $\textbf{Dendrogram}_Z$.

In this study, Z is set to 2 to find the connection cluster in the specific brain area associated with fatigue. As shown in Fig. 4, two clusters are left by the second level cut. The single-element cluster C_5 corresponding to node 5 is extracted in this exemplar dendrogram. The node correspond to the EEG electrode, wherefore the clustering process is also an EEG dimensionality reduction process of which results can also be applied to the following processes of fatigue detection.

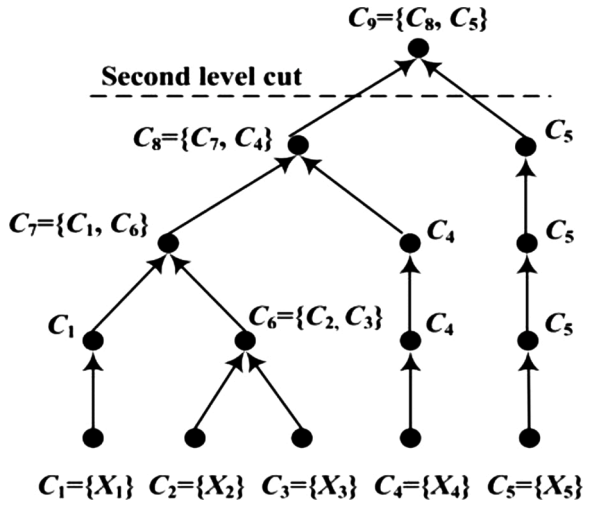

Fig. 4. An exemplar dendrogram representing a possible hierarchical clustering process for 5 connection clusters.

2.4. Spatio-temporal imaging

To quantify the complexity of EEG activity dynamically during driving, the wavelet entropy features showing effectiveness in [4] and [5] were extracted in a sliding window ($L = 30$*sampling length). With the application of wavelet decomposition in the experimental data preprocessing, the probability distribution p_x in the entropy calculation was derived from the energy distribution of wavelet coefficients in the sliding window (see details in [5]). The wavelet entropy in the ith sliding window was represented by

$$WE_i = -\sum_x p_x \bullet \log(p_x) \tag{8}$$

where x denotes the resolution level of wavelet decomposition, which may correspond to any of the wavelet coefficient group, i.e. delta, theta, alpha, and beta.

When we focus on the specific connection clusters (specific nodes) on brain networks, the clustering method actually plays a role in sparse representation of the spatial domain for adapting to dynamic feature extraction during prolonged driving. Now we have not only spatial information reflected by the key nodes (corresponding to the extracted clusters), but also temporal information reflected by the dynamic entropy features. The temporal features integrated with clustering result on brain networks in Fig. 1 are represented as 2D images (feature matrices in Fig. 5). The value of each pixel $\boldsymbol{I}_p$ (i, j)=$\boldsymbol{WE}$(i, j) represents the wavelet entropy value of subject p at the jth key spatial node ($j = 1,2, \ldots m$) and in ith sliding window ($i = 1,2,\ldots t$).

We analyzed the feature data through digital image processing in order to visualize their patterns and to distinguish these patterns (see Sec. *E*). The image processing techniques are mainly about the edge detection of spatial values of the measured feature field at t-y, $\boldsymbol{I}(t, y)$, at each subject p, (i.e., 2D image processing).

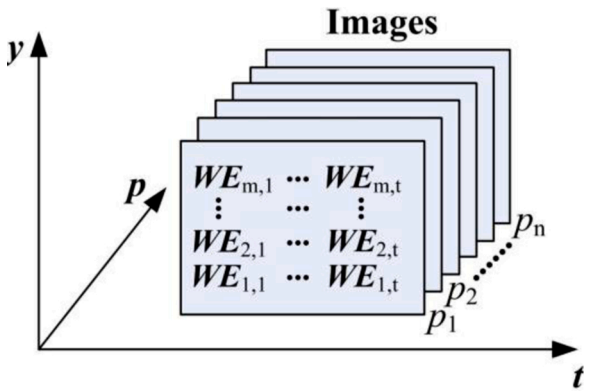

Fig. 5. Sequence of feature matrices.

2.5. Two-dimensional pattern recognition

Fatigue detection usually requires pattern differentiation in the time domain to facilitate application and feedback (i.e. warning). After feature imaging, the entropy-based features are represented by the 2D images with reduced spatial fluctuations. Here, we employed pulse-coupled neural networks (PCNN) to find the time point of onset of EEG pattern change and to differentiate different brain states.

In 1990, Eckhorn proposed linking field network model based on the phenomenon of synchronous pulse bursts in the visual cortices of cats [34], after which Johnson brought forward the PCNN model [35,36]. PCNN has been successfully applied to many areas of image processing, such as image segmentation [37] and object detection [38]. Since the basic PCNN model is relatively complex, a simplified PCNN is frequently used. The simplified PCNN model consists of three functional units: the dendrite tree, the linking modulation, and the pulse generator, see Fig. 6.

The PCNN neuron receives inputs from two different fields: other neurons and external sources (here they are the images from Sec. *D*). Thus there are two branches on the dendrite tree corresponding to the feeding input $\boldsymbol{F}_{ij}$ and the linking input $\boldsymbol{L}_{ij}$, respectively. The linking modulation couples the feedback and linking inputs to constitute the internal activity $\boldsymbol{U}_j$ of the neuron. In the pulse generator, the output Y is generated by comparing the internal activity with the neuron's dynamic threshold. If the internal activity is strong enough, the neuron will be activated (i.e., the output $Y=1$). Then output feedback increases the threshold and the neuron is inhibited (i.e., the output $Y=0$). Therefore, the neuron generates a pulse. The pulse signals are outputted to the adjacent neurons and affect their activation state [39].

The PCNN structure can be described by the following discrete equations:

$$F_{ij}[n] = I_{ij} \tag{9}$$

$$L_{ij}[n] = \mathrm{e}^{-\alpha_L} L_{ij}[n-1] + V_L \sum_{k,l} M_{ijkl} Y_{kl}[n-1] \tag{10}$$

$$U_{ij}[n] = F_{ij}[n]\left(1 + \beta L_{ij}[n]\right) \tag{11}$$

$$\theta_{ij}[n] = \mathrm{e}^{-\alpha_\theta} \theta_{ij}[n-1] + V_\theta Y_{ij}[n-1] \tag{12}$$

$$Y_{ij}[n] = \begin{cases} 1 & U_{ij}[n] \geq \theta_{ij}[n] \\ 0 & U_{ij}[n] < \theta_{ij}[n] \end{cases} \tag{13}$$

$$M_{ij} = \frac{1}{(i-k)^2 + (j-l)^2} \tag{14}$$

The (i, j) pair stands for the position of the neuron in the map. The (k, l) pair stands for the position of the neighbor neuron. Eqs. (9) and (10) represent a dendrite tree where $\boldsymbol{I}_{ij}$ is the external stimulus (input) and $\boldsymbol{M}_{ijkl}$ synaptic weight coefficients. $\boldsymbol{M}$ can be calculated by Eq. (14). F and L are called feeding and linking functions. α_L is the time decay constants for linking and feeding. V_L is the area amplification factors for linking and feeding. Eq. (11) is the linking modulation where β is the linking parameter and $\boldsymbol{U}_{ij}[n]$ represents the internal neuron state. The pulse generator is expressed in Eqs. (12) and (13) where $\boldsymbol{Y}_{ij}[n]$ represents the firing events depending on the internal neuron's state and dynamic threshold. The neuron dynamic threshold is calculated in Eq. (12), which indicates this system is a non-linear system. α_θ is the dynamic threshold constant and V_θ is the amplification factor.

For each subject p, its 2D matrix after clustering in Fig. 5 was put into PCNN as the external stimulus $\boldsymbol{I}_{ij}$. Through the pulse generator, the edges of different feature patterns can be obtained by the responses of the neuron discharges.

3. Results

3.1. Clustering on brain networks

Considering fatigue's impact on the functional interaction, the brain networks in three temporal stages of driving were constructed to extract the spatial features. Fig. 7(a) shows the spatial connectivity averaged across the subjects at the stages A (0 h), B (0.5 h), and C (1 h). The strengths of the edges were represented by the thickness of the edges (the larger the strength the thicker the line). In order to make the results more obvious, all the edge strengths were magnified up to 2 times. It can be observed that the overall functional connectivity at the stage C becomes obviously weaker with the accumulation of fatigue. The energy of all the elements in functional connectivity matrix $\boldsymbol{A}$ was calculated to obtain a measure for the overall connectivity strengths in every brain network. There is no statistical difference of the energy between the three stages (Wilconxon rank-sum test: $p > 0.05$). The larger p values between stages A and C and between stages B and C indicated the larger individual differences at stage C. Fig. 7(b) shows the alpha band power averaged across the channels and subjects at the stages A, B, and C. In contrast to the connectivity, the averaged alpha band power at different stages reveals an increase of alpha level with the accumulation of fatigue. However, the standard error of the alpha band power also increased during increase of fatigue and no significant differences of alpha band power were observed between the three stages.

Under the condition of no significantly statistical difference using the traditional connectivity and oscillation analyses, CBNs was applied to mining the spatiotemporal information. With clustering, the spatial nodes of the brain networks in Fig. 7(a) were classified into two groups and the deep blue nodes whose attributes were 'farthest' from others

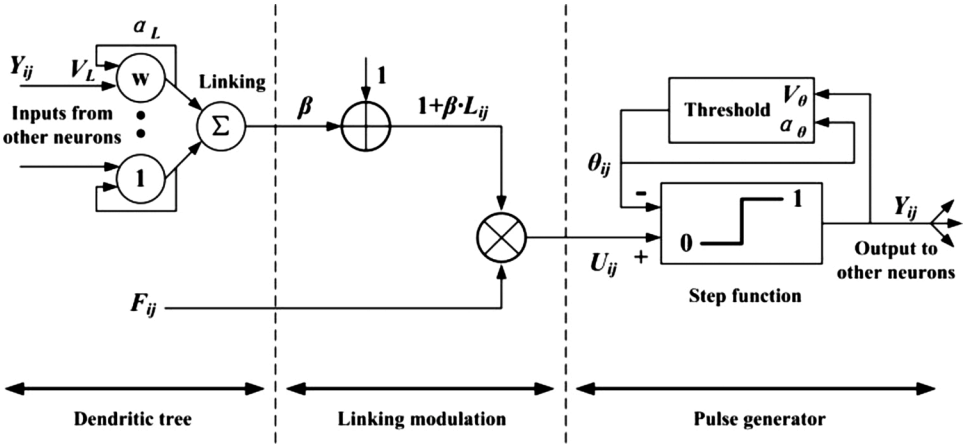

Fig. 6. PCNN neuron model.

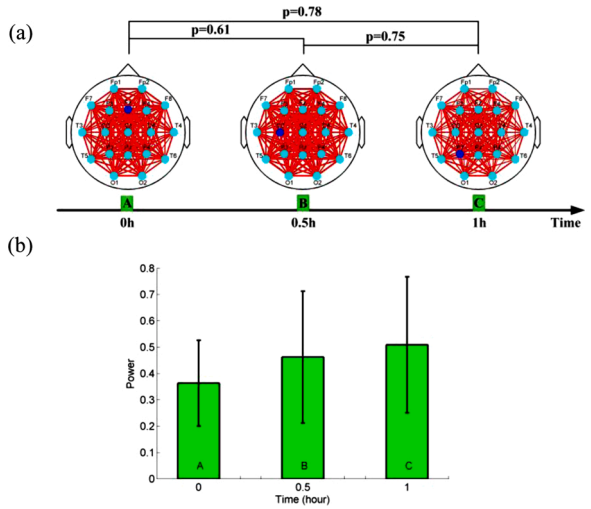

Fig. 7. Connectivity and oscillation power changes. (a) Averaged functional brain networks at the stages A, B, and C. (b) Averaged power in alpha band.

were obtained by using (3)-(7). The outstanding nodes extracted based on the distance of functional connectivity in alpha band evolve across three brain functional areas (i.e. frontal, central, and parietal regions), which shows a gradient distribution feature in the space domain with the accumulation of fatigue. Since more distinct connectivity corresponds to larger distance, the clustering results suggest that the alpha oscillation gather in posterior brain region during states of fatigue.

3.2. Spatio-temporal imaging

Fig. 8(a) presents the dynamic entropy features of all the EEG channels. The stage changes and degraded performance of the features mentioned in the literature of Sec. I are not clear enough for the different spatial loci of EEG recordings. Because of signal mixing, the fluctuations blur the critical point (turning-point corresponding to subjective fatigue) position, which is important labeling information of fatigue. As shown in Fig. 8(b), the temporal features from the nodes obtained by CBNs have more easily distinguishable synchronization changes. It can be observed that the entropy values change significantly after about 28 min.. As the probability distribution of event occurrence is represented by the energy distribution of different kinds of alpha activities, the entropy value decreasing reveals activity complexity reducing. Consequently, the subject probably enters a deeper stage of fatigue after

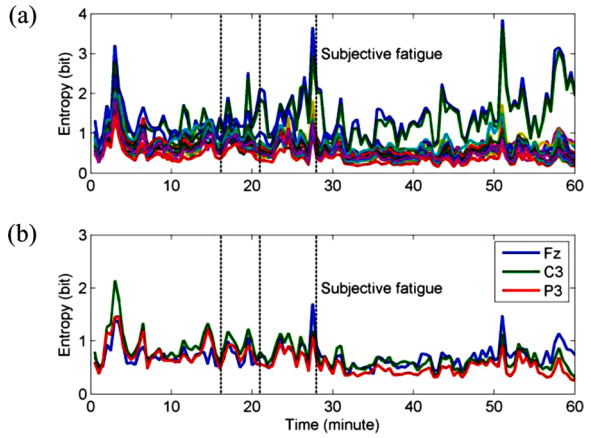

Fig. 8. Dynamic entropy features of a subject. (a) Wavelet entropy extracted from all the 19 channels. (b) Wavelet entropy extracted from the nodes obtained by clustering on the brain network.

the critical point. This is supported by the records of subjectively reported levels of fatigue in the experiment. As shown in the first row of Table 1, the critical point in Fig. 8 corresponds to the third point marked by the subject. It seems that there are more fatigue stages in fact than observation. The results reflect different levels of fatigue and individual differences are obtained in the next section.

3.3. Two-dimensional pattern recognition

To further distinguish different levels of fatigue automatically, the EEG features with the optimized spatial information for each subject were represented as 2D matrix. Fig. 9(a) shows the 2D image corresponding to the matrix of the EEG features in Fig. 8(b). The three rows of pixels in the feature image indicate channels Fz (5th node), C3 (9th node), and P3 (14th node) respectively. The columns of pixels in the feature image depict the changes of wavelet entropy as a function of time in continuous driving. The feature values were normalized and represented by different colors. Hence color gradients in the time domain reveal fatigue accumulation and retain stage changes in different rows. The blocks containing wide range of pixels in the similar color are observable, a red block emerging after about 28 min. striking as the most obvious. It corresponds to fatigue level 3 in Table 1.

Fig. 9(b) and (c) present the results of the PCNN recognition. Because the model neurons' activated and inhibited states are induced by the stage changes of different features, the generated pulses segment the 2D image and the red blocks are identified. If we just focus on the independent red pulses in Fig. 9(b), they happen to be at the edges of different patterns (see Fig. 9(c)). The black pulses in Fig. 9(c) correspond to the independent red pulses in Fig. 9(b). Since the exact time of the pulse generation is also recorded in the image, the fatigue time can be obtained from the EEG analysis to differentiate different stages during driving and it is shown in the third row of Table 1. Comparing the second row with the third row in Table 1, the pulses reflecting the excitability and inhibition changes of the PCNN neurons are concordant with subjective feelings of fatigue to an extent. Especially around the block with the widest range, the EEG-based detection has the best effect on estimating the deepening of the fatigue, because the time determined by PCNN is near and before the time marked by the subjects. At that stage, the PCNN neurons are inhibited for a long time ($Y = 0$ in Fig. 9(b) and (c)).

In Fig. 10(a), which shows the results of all the different subjects' detection based on the extracted nodes (the deep blue nodes in Fig. 7 (a)), all the individual subjective and objective turning points of fatigue are visible. To quantify these results, the physiological outputs' time errors from the subjective judgments were calculated and are shown in Fig. 10(b). Since the physiological outputs were used as minuends, the points below the x-axis (zero error) indicate such situation that the time of fatigue from the physiological detection is before the time of fatigue from the subjective response. In total, 16 out of 26 error points in Fig. 10 (b) are below the x-axis, which means most fatigue-related points obtained by the two-dimensional pattern recognition in Fig. 10(a) can not only match the points where the subjects start to feel fatigued, but also precede these. For all the subjects, there were a total of 29 accidents happened in the simulated driving task. Twenty one accidents occurred after the detected fatigue in Fig. 10.

To compare with the fatigue detection performance of existing methods, the last critical time point of each subject is used as the cut-off point to give two category labels to calculate the classification accuracy of fatigue. As shown in Table 2, the average accuracy of all the subjects in this paper is 96.7 %. It achieves better detection performance compared with the state-of-the-art techniques mentioned in Section 1.

4. Discussion

The effects of fatigue are multifaceted [40]. It can bring the EEG changes in time-frequency-spatial domain. The results of the present

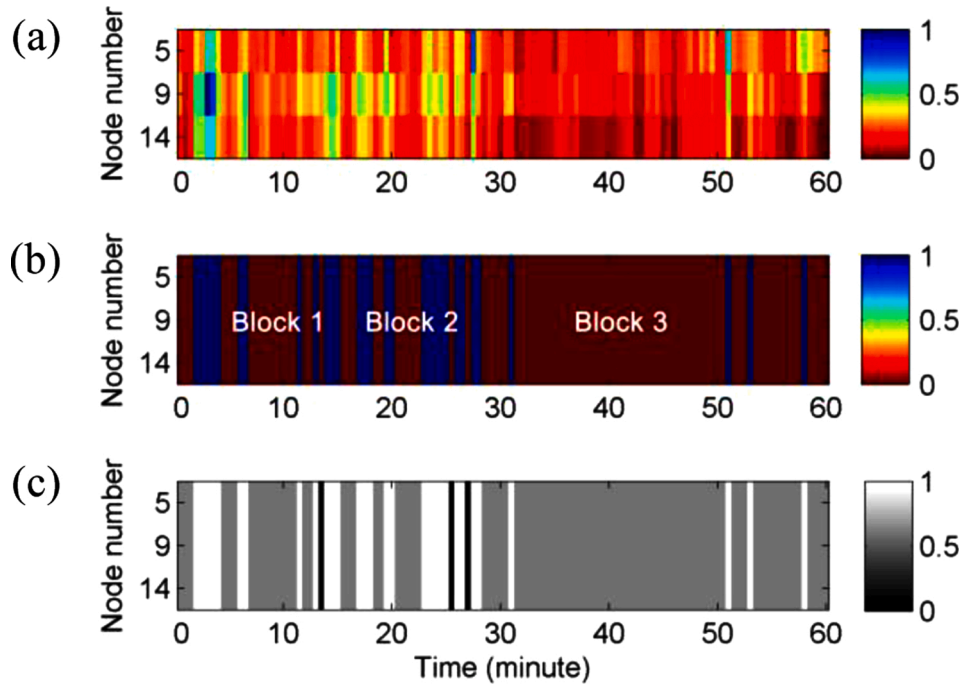

Fig. 9. Fatigue pattern recognition results of the subject. (a) Transformed image of EEG features. (b) PCNN outputs. (c) Edge detection.

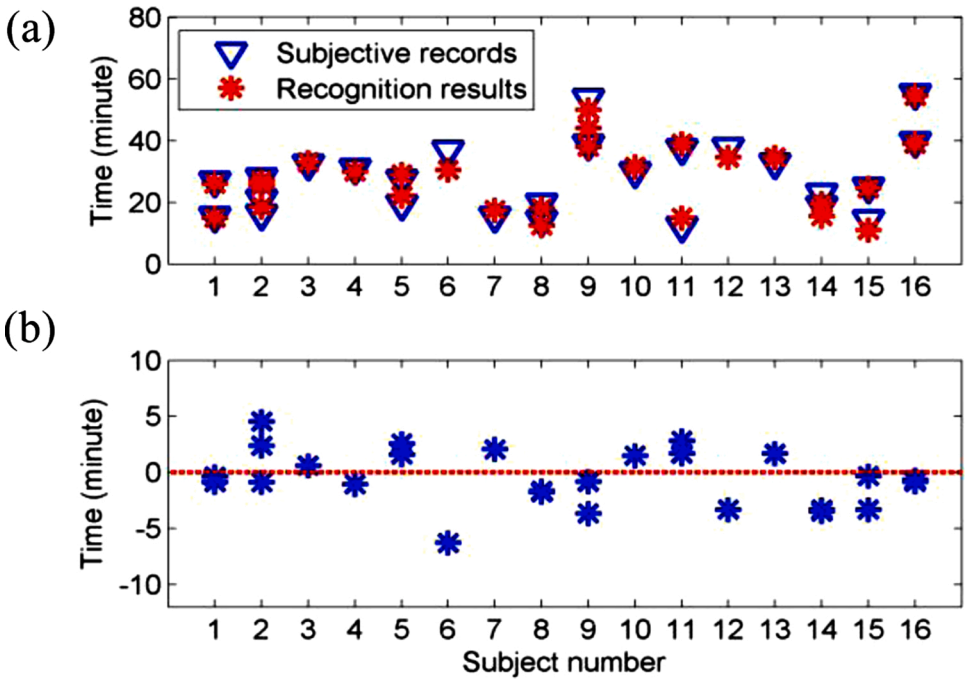

Fig. 10. Comparison of critical time points between subjective reports and objective detection based on the extracted nodes. (a) Critical time points of subjective reports and objective detection. (b) Physiological outputs' time errors from subjective judgments.

study confirm the detection accuracy of fatigue can be further improved by introducing effective spatial information. The spatial information is extracted by CBNs.

Due to the issues such as signal mixing, the spatial information is vulnerable to interference, which needs to be processed. Especially in the prolonged driving task, the fatigue-related information was not only easily implied, but also with unnecessary redundancy or fluctuations. As shown in Fig. 7(b), the variance (fluctuation) among different channels and subjects became larger with the accumulation of fatigue, even though the mean alpha level increased. The individual differences including channels and subjects might severely affect the assessment for fatigue, since there were no significant differences of alpha band power between the three stages A, B, and C. As shown in Fig. 7(a), the decreased connectivity also has no statistical significance ($p > 0.05$). Note that all subjects in the experiments expressed the subjective feelings of fatigue (see Fig. 10). Under the influence of various sensory and cognitive processes operating during driving, the existence probability of the information redundancy also increased among all the nodes (see Fig. 8(a)).

Therefore, the clustering algorithm was used to visualize space

Table 2
Classification accuracy comparison of the previous works.

Research group	Feature extraction	Classifier	Accuracy (%)
Li et al. [13]	Power spectra ratio indices	Linear regression	91.5
Lawhern [14]	Alpha spindle	DAR model	95.0 %
Khushaba et al. [17]	FE	LDA, kNN, and SVM	92.8
Luo et al. [19]	Adaptive multi-scale FE	SVM	95.4
Wang et al. [18]	WE	SVM	90.7
Zhang et al. [5]	WE, ApEn, and SampEn	MLP	96.5
This paper	CBNs-WE	PCNN	96.7

distribution features in fewer significant nodes. It distinguished the special nodes with distinct connectivity attributes throughout the networks. If we project the spatial information to the time dimension again, the clustered node sources indicating enriched alpha activities move from the frontal region to the parietal region while the fatigue deepens. As each clustered source corresponds to a node, the algorithm actually achieves sparse representation and reduces the information redundancy in the space domain. Fatigue influences the specific synchrony form among alpha signals (i.e. clusters) and brings the variations of the space distribution features (from the frontal region to the parietal region). The results of the present study are consistent with the previous studies where oscillatory activity at alpha band has been observed to increase in the posterior brain regions (parietal-occipital) during attentional lapses [41] and during states of drowsiness relative to states of alertness [8,42]. In addition, as is well known, each hemisphere of the brain controls the opposite side of the body. Accordingly, the changes of the alpha enrichment area from the frontal region to the parietal region were with lateral offset. It is interesting to note that in this right handed subject population, the clustering outputs reflected significance of especially the left hemisphere sensors (C3 and P3).

Moreover, the improvement of the EEG imaging effect compared to earlier approaches comes from multiple perspectives. In the time domain, the critical points between the significantly different stages have practical significance, for they can become early triggers of feedback warnings. As shown in Fig. 8, the temporal features extracted from the clustered nodes had more distinct changes in synchronization than those from all the nodes, especially at the critical point of self-reported deepest level of fatigue. This also indicates that the compression of spatial information by clustering is effective. It is obvious that the amount of calculation will be reduced after the identification of the significant nodes, which are sparse. In consideration of clustering on brain networks, dynamic features over larger time frames can be efficiently extracted. This provides the possibility for the subsequent two-dimensional pattern recognition and imaging interpretation.

As a measure of average uncertainty of event set [43], the entropy-based features visualized the fatigued-related information in the time domain. Decreasing entropy value reflects decreasing complexity of brain activities [5]. Our data are in line with the literature reporting functional segregation of neuronal assemblies in anterior and posterior regions during the transition between stages of fatigue [44]. Our results should contribute to understanding of complex reorganization of the cortical distribution of alpha oscillations during the wake/-drowsy transition. With low entropy value there is less choice, or uncertainty, when there are less possible events. The less alternating brain activities reflect a condition where only the most important function areas will stay relatively active after the drivers are fatigued. In the prolonged driving task, there always EEG features on a few nodes retain the overall trend (Fig. 8). Thus, it could also reflect a state where the brain information processing is not influenced by environmental factors, and the processed signaling reflects more ‘self-genrated’ or ‘self-paced’ processing. This may explain the gradient changes of the temporal features in Fig. 9. It is well known that drowsiness proceeds in stages [45]. Prior publications suggest that fatigue can considerably influence topographic distribution of EEG alpha attractor correlation dimension values [44]. Additionally, the reactivity to external stimulation varies considerably and positive reactions decrease in the course of the development of fatigue [46,47]. Compared to Fig. 8(a), Fig. 8(b) shows a clearer downward trend. From the perspective of fatigue detection, simply increasing the number of the electrodes (nodes) will degrade the performance of the system, because not all the electrodes are significant. The spatial information covering the entire brain may be redundant due to signal mixing. In this study, the significant electrodes are automatically obtained by the clustering algorithm implemented in brain networks.

Since both the extracted spatial and temporal information was found useful, the temporal features on all the selected nodes were converted into images to visualize the fatigue patterns. As shown in Fig. 9, the space-time matrix outputted different color blocks corresponding to different patterns. Therefore two-dimensional pattern recognition can also be considered as an edge detection technique for image segmentation to find the critical points of fatigue. Based on the discharge responses of PCNN, the observable blocks (in Fig. 9(a)) were recognized (in Fig. 9(b) and (c)) and the critical points were obtained. Compared with the existing methods of fatigue detection in Table 2, the higher classification performance confirms the effectiveness of the proposed method of spatiotemporal imaging analysis.

To ensure that the detected fatigue is the real fatigue felt by the subjects, we simultaneously measured subjective and physiological responses and quantified their differences through the critical time points of self-reported and detected fatigue. As shown in Table 1 and Fig. 10, the discharge responses of PCNN neurons had a good concordance with subjective responses. The prolonged non-active state (red blocks $Y = 0$) of PCNN neurons reflects the prolonged lack of complex activities and the consistency change of different brain areas within intermediate frontal, central (motor-sensory), and parietal regions represented as the three extracted nodes. If the brain functions of which they are responsible for are simultaneously not active while driving, this will have severe consequences for traffic safety. Kaplan et al. have proven that the subjects in drowsiness state have ability to predict sleep onset [48]. However when the fatigue is deeper, the objective physiological measures will become more significant, because drivers may not be willing to give any extra response when they are fatigued in real-world situations. In the experiments, 21 of 29 accidents happened after detected fatigue. These accidents probably were caused by driver fatigue. Further, most detected times of fatigue in Fig. 10 occurred before the times of fatigue reported by the subjects. This indicates subjective fatigue is closer to the accidents. The proposed method is extremely useful for early warning feedback or other fatigue countermeasures in practical applications.

5. Conclusion

In this paper, a new EEG imaging method for automated detection and identification of driver fatigue was proposed. The nonlinear dynamical features of EEG from spatially optimized nodes extracted by CBNs were transformed into spatio-temporal images to extract reliably critical information of fatigue. The PCNN-based image processing method was utilized to recognize the two-dimensional fatigue pattern. The results showed that the temporal features from the spatially optimized nodes keep fatigue information and reduce the fluctuations in space. Most of the detected fatigue points not only kept a good concordance with the subjective fatigue points, but also occurred before accidents, which shows the effectiveness of the proposed method and its promise for enabling early warning applications for fatigue.

CRediT authorship contribution statement

Chi Zhang: Conceptualization, Methodology, Software,

Visualization, Writing - original draft, Writing - review & editing. **Lina Sun:** Conceptualization, Writing - original draft, Writing - review & editing. **Fengyu Cong:** Supervision. **Tuomo Kujala:** Resources, Writing - review & editing, Supervision. **Tapani Ristaniemi:** Conceptualization, Supervision. **Tiina Parviainen:** Writing - review & editing, Supervision.

Declaration of Competing Interest

The authors declare that they have no known competing financial interests or personal relationships that could have appeared to influence the work reported in this paper.

Acknowledgments

This work was supported by the National Natural Science Foundation of China (grant number 61703069), the National Foundation in China (No. JCKY2019110B009), and the Fundamental Research Funds for the Central Universities [grant number DUT18RC(4)035]. It is also to memorize Prof. Tapani Ristaniemi for his great help to Fengyu Cong and Chi Zhang.

References

[1] M. Jagannath, V. Balasubramanian, Assessment of early onset of driver fatigue using multimodal fatigue measures in a static simulator, Appl. Ergon. 45 (2014) 1140–1147.
[2] F. Siddiqui, Z. Siddiqui, T. Khan, F. Shaikh, Simulation of driver drowsiness detection technique, Imperial J. Interdiscip. Res. 2 (2016) 140–143.
[3] Asleep at the Wheel: a National Compendium of Efforts to Eliminate Drowsy Driving, NHTSA, Washington, D.C., U.S, 2017.
[4] S. Kar, M. Bhagat, A. Routray, EEG signal analysis for the assessment and quantification of driver's fatigue, Transp. Res. Part F Traffic Psychol. Behav. 13 (2010) 297–306.
[5] C. Zhang, H. Wang, R. Fu, Automated detection of driver fatigue based on entropy and complexity measures, IEEE Trans. Intell. Transp. Syst. 15 (2014) 168–177.
[6] S.K. Lal, A. Craig, Driver fatigue: electroencephalography and psychological assessment, Psychophysiology 39 (2002) 313–321.
[7] R. Fu, H. Wang, W. Zhao, Dynamic driver fatigue detection using hidden Markov model in real driving condition, Expert Syst. Appl. 63 (2016) 397–411.
[8] M. Simon, E.A. Schmidt, W.E. Kincses, M. Fritzsche, A. Bruns, C. Aufmuth, M. Bogdan, W. Rosenstiel, M. Schrauf, EEG alpha spindle measures as indicators of driver fatigue under real traffic conditions, Clin. Neurophysiol. 122 (2011) 1168–1178.
[9] G. Borghini, G. Vecchiato, J. Toppi, L. Astolfi, A. Maglione, R. Isabella, C. Caltagirone, W. Kong, D. Wei, Z. Zhou, Assessment of mental fatigue during car driving by using high resolution EEG activity and neurophysiologic indices, Engineering in Medicine and Biology Society (EMBC), in: 2012 Annual International Conference of the IEEE, IEEE, 2012, pp. 6442–6445.
[10] L. De Gennaro, M. Ferrara, G. Curcio, R. Cristiani, Antero-posterior EEG changes during the wakefulness–sleep transition, Clin. Neurophysiol. 112 (2001) 1901–1911.
[11] H. Tanaka, M. Hayashi, T. Hori, Statistical features of hypnagogic EEG measured by a new scoring system, Sleep 19 (1996) 731–738.
[12] S. Charbonnier, R.N. Roy, S. Bonnet, A. Campagne, EEG index for control operators' mental fatigue monitoring using interactions between brain regions, Expert Syst. Appl. 52 (2016) 91–98.
[13] W. Li, Q.-c. He, X.-m. Fan, Z.-m. Fei, Evaluation of driver fatigue on two channels of EEG data, Neurosci. Lett. 506 (2012) 235–239.
[14] V. Lawhern, S. Kerick, K.A. Robbins, Detecting alpha spindle events in EEG time series using adaptive autoregressive models, BMC Neurosci. 14 (2013) 101.
[15] L.-C. Shi, Y.-Y. Jiao, B.-L. Lu, Differential entropy feature for EEG-based vigilance estimation, Engineering in Medicine and Biology Society (EMBC), in: 2013 35th Annual International Conference of the IEEE, IEEE, 2013, pp. 6627–6630.
[16] L.-l. Chen, Y. Zhao, J. Zhang, J.-z. Zou, Automatic detection of alertness/drowsiness from physiological signals using wavelet-based nonlinear features and machine learning, Expert Syst. Appl. 42 (2015) 7344–7355.
[17] R.N. Khushaba, S. Kodagoda, S. Lal, G. Dissanayake, Driver drowsiness classification using fuzzy wavelet-packet-based feature-extraction algorithm, IEEE Trans. Biomed. Eng. 58 (2011) 121–131.
[18] Q. Wang, Y. Li, X. Liu, Analysis of feature fatigue EEG signals based on wavelet entropy, Intern. J. Pattern Recognit. Artif. Intell. 32 (2018).
[19] H. Luo, T. Qiu, C. Liu, P. Huang, Research on fatigue driving detection using forehead EEG based on adaptive multi-scale entropy, Biomed. Signal Process. Control 51 (2019) 50–58.
[20] G.H. Klem, H.O. Luders, H.H. Jasper, C. Elger, The ten-twenty electrode system of the International Federation. The International Federation of Clinical Neurophysiology, electroencephalography and clinical neurophysiology, Supplement 52 (1999) 3–6.
[21] C.-H. Chuang, C.-S. Huang, L.-W. Ko, C.-T. Lin, An EEG-based perceptual function integration network for application to drowsy driving, Knowledge Based Syst. 80 (2015) 143–152.
[22] C. Imperatori, B. Farina, M. Adenzato, E.M. Valenti, C. Murgia, G.D. Marca, R. Brunetti, E. Fontana, R.B. Ardito, Default mode network alterations in individuals with high-trait-anxiety: an EEG functional connectivity study, J. Affect. Disord. 246 (2019) 611–618.
[23] Y. Sun, J. Lim, K. Kwok, A. Bezerianos, Functional cortical connectivity analysis of mental fatigue unmasks hemispheric asymmetry and changes in small-world networks, Brain Cogn. 85 (2014) 220–230.
[24] P. Qi, H. Ru, L. Gao, X. Zhang, T. Zhou, Y. Tian, N. Thakor, A. Bezerianos, J. Li, Y. Sun, Neural mechanisms of mental fatigue revisited: new insights from the brain connectome, Engineering 5 (2019) 276–286.
[25] G. Gaggioni, J.Q.M. Ly, S.L. Chellappa, D. Coppieters 't Wallant, M. Rosanova, S. Sarasso, A. Luxen, E. Salmon, B. Middleton, M. Massimini, C. Schmidt, A. Casali, C. Phillips, G. Vandewalle, Human fronto-parietal response scattering subserves vigilance at night, NeuroImage 175 (2018) 354–364.
[26] W. Kong, W. Lin, F. Babiloni, S. Hu, G. Borghini, Investigating driver fatigue versus alertness using the granger causality network, Sensors 15 (2015) 19181–19198.
[27] C. Zhao, M. Zhao, Y. Yang, J. Gao, N. Rao, P. Lin, The reorganization of human brain networks modulated by driving mental fatigue, IEEE J. Biomed. Health Inform. 21 (2017) 743–755.
[28] J.M. Palva, S.H. Wang, S. Palva, A. Zhigalov, S. Monto, M.J. Brookes, J.-M. Schoffelen, K. Jerbi, Ghost interactions in MEG/EEG source space: a note of caution on inter-areal coupling measures, Neuroimage 173 (2018) 632–643.
[29] S.H. Wang, M. Lobier, F. Siebenhühner, T. Puoliväli, S. Palva, J.M. Palva, Hyperedge bundling: a practical solution to spurious interactions in MEG/EEG source connectivity analyses, Neuroimage 173 (2018) 610–622.
[30] E.M. Nowara, T.K. Marks, H. Mansour, A. Veeraraghavan, SparsePPG: towards driver monitoring using camera-based vital signs estimation in near-infrared, 2018 IEEE/CVF Conference on Computer Vision and Pattern Recognition Workshops (CVPRW) (2018) 1353–135309.
[31] U. Kalabić, A. Chakrabarty, R. Quirynen, S.D. Cairano, Learning autonomous vehicle passengers' preferred driving styles using g-g plots and haptic feedback, 2019 IEEE Intelligent Transportation Systems Conference (ITSC) (2019) 4012–4017.
[32] H. Onias, A. Viol, F. Palhano-Fontes, K.C. Andrade, M. Sturzbecher, G. Viswanathan, D.B. de Araujo, Brain complex network analysis by means of resting state fMRI and graph analysis: will it be helpful in clinical epilepsy? Epilepsy Behav. 38 (2014) 71–80.
[33] M.-T. Horstmann, S. Bialonski, N. Noennig, H. Mai, J. Prusseit, J. Wellmer, H. Hinrichs, K. Lehnertz, State dependent properties of epileptic brain networks: comparative graph–theoretical analyses of simultaneously recorded EEG and MEG, Clin. Neurophysiol. 121 (2010) 172–185.
[34] R. Eckhorn, H.J. Reitboeck, M. Arndt, P. Dicke, Feature linking via synchronization among distributed assemblies: simulations of results from cat visual cortex, Neural Comput. 2 (1990) 293–307.
[35] D. Zhou, R. Nie, D. Zhao, Analysis of autowave characteristics for competitive pulse coupled neural network and its application, Neurocomputing 72 (2009) 2331–2336.
[36] J.L. Johnson, M.L. Padgett, PCNN models and applications, IEEE Trans. Neural Netw. 10 (1999) 480–498.
[37] H. Berg, R. Olsson, T. Lindblad, J. Chilo, Automatic design of pulse coupled neurons for image segmentation, Neurocomputing 71 (2008) 1980–1993.
[38] H.S. Ranganath, G. Kuntimad, Object detection using pulse coupled neural networks, IEEE Trans. Neural Netw. 10 (1999) 615–620.
[39] R.C. Mureşan, Pattern recognition using pulse-coupled neural networks and discrete Fourier transforms, Neurocomputing 51 (2003) 487–493.
[40] J.F. Hopstaken, D. Linden, A.B. Bakker, M.A. Kompier, A multifaceted investigation of the link between mental fatigue and task disengagement, Psychophysiology 52 (2015) 305–315.
[41] M.T. Peiris, P.R. Davidson, P.J. Bones, R.D. Jones, Detection of lapses in responsiveness from the EEG, J. Neural Eng. 8 (2011) 1–15.
[42] V. Lawhern, S. Kerick, K.A. Robbins, Detecting alpha spindle events in EEG time series using adaptive autoregressive models, BMC Neurosci. 14 (2013) 1–16.
[43] C.E. Shannon, A mathematical theory of communication, ACM Sigmobile Mob. Comput. Commun. Rev. 5 (1948) 3–55.
[44] A. Kalauzi, A. Vuckovic, T. Bojić, Topographic distribution of EEG alpha attractor correlation dimension values in wake and drowsy states in humans, Int. J. Psychophysiol. 95 (2015) 278–291.
[45] T. Hori, M. Hayashi, T. Morikawa, Topographical EEG Changes and the Hypnagogic Experience, 1994.
[46] J. Minkwitz, M.U. Trenner, C. Sander, S. Olbrich, A.J. Sheldrick, U. Hegerl, H. Himmerich, Time perception at different EEG-vigilance levels, Behav. Brain Funct. 8 (2012) 50.
[47] B. Roth, The clinical and theoretical importance of EEG rhythms corresponding to states of lowered vigilance, Electroencephalogr. Clin. Neurophysiol. 13 (1961) 395–399.
[48] K.A. Kaplan, A. Itoi, W.C. Dement, Awareness of sleepiness and ability to predict sleep onset: can drivers avoid falling asleep at the wheel? Sleep Med. 9 (2007) 71–79.